

Spin-triplet Supercurrent through Inhomogeneous Ferromagnetic Trilayers

Mohammad Alidoust¹ and Jacob Linder¹

¹*Department of Physics, Norwegian University of Science and Technology, N-7491 Trondheim, Norway*

(Dated: February 19, 2011)

Motivated by a recent experiment [J. W. A. Robinson, J. D. S. Witt and M. G. Blamire, *Science*, **329**, 5987 (2010)], we here study the possibility of establishing a long-range spin-triplet supercurrent through an inhomogeneous ferromagnetic region consisting of a Ho|Co|Ho trilayer sandwiched between two conventional *s*-wave superconductors. We utilize a full numerical solution in the diffusive regime of transport and study the behavior of the supercurrent for various experimentally relevant configurations of the ferromagnetic trilayer. We obtain qualitatively very good agreement with experimental data regarding the behavior of the supercurrent as a function of the width of the Co-layer, L_{Co} . Moreover, we find a synthesis of $0-\pi$ oscillations with superimposed rapid oscillations when varying the width of the Ho-layer which pertain specifically to the spiral magnetization texture in Ho. We are not able to reproduce the anomalous peaks in the supercurrent observed experimentally in this regime, but note that the results obtained are quite sensitive to the exact magnetization profile in the Ho-layers, which could be the reason for the discrepancy between our model and the experimental reported data for this particular aspect. We also investigate the supercurrent in a system where the intrinsically inhomogeneous Ho ferromagnets are replaced with domain-wall ferromagnets, and find similar behavior as in the Ho|Co|Ho case. Furthermore, we propose a novel type of magnetic Josephson junction including only a domain-wall ferromagnet and a homogeneous ferromagnetic layer, which in addition to simplicity regarding the magnetization profile also offers a tunable long-range spin-triplet supercurrent. Finally, we discuss some experimental aspects of our findings.

PACS numbers: 74.45.+c, 74.50.+r, 75.70.Cn, 74.20.Rp, 74.78.Na

1. INTRODUCTION

Due to the rich physics from a fundamental viewpoint and the possibility of birthing practical applications, configurations containing superconductors and ferromagnets have attracted much attention theoretically^{4-8,11,12} and experimentally^{1-3,9,10,13-15} over the last years (see for instance Ref. 2 for a comprehensive review and reference-list). One of the most intriguing phenomena in the context of this interplay is the generation of a long-ranged spin-triplet supercurrent flowing through a Josephson junction with magnetic elements. The main criterion for generation of such a current is that some form of magnetic inhomogeneity must be present in the junction, as first shown by Bergeret *et al.*²⁰⁻²² and Volkov *et al.*²³⁻²⁵. In the diffusive limit of transport, being often the experimentally most relevant regime, such a non-uniform magnetization can induce exotic long-range superconducting correlations which are odd under time-reversal: the so-called odd-frequency superconducting state. The resulting triplet-supercurrent decays over same length scale as in a superconductor|normal metal|superconductor (S|N|S) junction, but now additionally activates the spin-degree of freedom in the transport of Cooper pairs. A long-range triplet-supercurrent was predicted to occur in a setup consisting of three non-collinear homogeneous magnetic layers¹⁵, but disappears in the scenario of only two homogeneous non-collinear magnetic layers, as discussed in Refs. 26,35,38,39. Over the last couple of years, induction of triplet-correlations in layered heterostructures with ferromagnets (F) and superconductors (S) in the clean limit has been studied by using different formalisms and configurations in Refs. 40-42. On the experimental side, Keizer *et al.*⁴⁴ observed a long-range supercurrent through half-metallic CrO₂, whereas very recent

work also reports observation of a long-range supercurrent through an inhomogeneous magnetic layer^{6,27}. In particular, Robinson *et al.*³⁵ investigated the appearance of a spin-triplet supercurrent flowing through a magnetic Ho|Co|Ho trilayer. Due to the intrinsic magnetic inhomogeneity in Ho, featuring a spiral magnetization texture, it was found that a strong spin-triplet supercurrent was established through the trilayer connecting two *s*-wave superconducting leads. In this paper, motivated by the very recent experimental in Ref. 35, we utilize a full numerical solution of the quasiclassical Green's function in the diffusive regime and study theoretically spin-triplet condensation in the critical charge current flowing through a Ho|Co|Ho magnetic trilayer. Due to our numerical approach, we have access to the full-proximity effect regime and complicated magnetization textures in the trilayer. This allows us to also study the influence of domain-walls in the ferromagnet on the behavior of the long-range supercurrent.

The main results in Ref. 35 due to Robinson *et al.* were (i) a slow decay of the supercurrent as a function of the Co-layer thickness and (ii) anomalous peaks arising in the characteristic voltage of the junction as a function of the Ho-layer thickness. Using the computational machinery described above, we obtain qualitatively very good agreement with the experimental data pertaining to (i). However, we are not able to reproduce the anomalous peaks observed for the supercurrent pertaining to (ii). Instead, we find a synthesis of $0-\pi$ oscillations with superimposed rapid oscillations which pertain specifically to the spiral magnetization texture in Ho. However, we also show how the exact behavior of the supercurrent vs. the width of the inhomogeneous magnetic layer is rather sensitive to the exact magnetization pattern. This suggests that the trilayer magnetization texture realized in the experiment by Robinson *et al.*³⁵ might differ somewhat from our model. Moti-

vated by the above mentioned reason, we also investigate how the critical current behaves when we replace the Ho layers in the trilayer junctions with domain-walls. Finally, we propose a novel type of inhomogeneous ferromagnetic Josephson junction with a simpler magnetization profile compared to previous proposals, including only a domain-wall and homogeneous ferromagnet, and demonstrate the possibility to tune the long-ranged spin-triplet supercurrent flowing through the junction.

This work is organized as follow: In Sec. 2, we present the main ingredients of the theory which is used throughout the paper, i.e. a quasiclassical Green's function method in the diffusive limit studied by means of the Usadel equation and supplemented with proper boundary conditions. In Sec. 3, we investigate the triplet-supercurrent flowing through an Ho|Co|Ho ferromagnetic trilayer as a function of both the Ho- and Co-layer thickness including two different magnetization textures in the Ho layers. In Sec. 4, we investigate how the behavior of the supercurrent is altered when the Ho regions are replaced with domain-wall ferromagnets, which also feature an intrinsic inhomogeneous magnetization texture. We also propose a novel type of ferromagnetic Josephson junctions to investigate the possibility of tuning the long-range contribution to the supercurrent via an external field. Finally, we summarize and give concluding remarks in Sec. 5.

2. THEORETICAL APPROACH

For studying various characteristics of different media, the Green's function method is a fundamental approach utilized in many areas of condensed-matter physics^{29,30}. In the context of non-equilibrium transport through different media one should start from Dyson's equation of motion and calculate the Keldysh Green's function³¹. In equilibrium situations, the Keldysh block of Green's function can be obtained from the Advanced and Retarded blocks of the Green's function. Inside superconducting regions, Dyson's equation of motion transforms to Gorkov's equations which in turn can be reduced to Eilenberger's equation within a quasiclassical approximation, where the Fermi wavelength is much smaller than all other length scales. The Eilenberger equation reads:³²

$$[E\hat{\tau}_3 + \hat{\Delta}, \hat{G}] + i\mathbf{v}_F \cdot \nabla \hat{G} - [\hat{\Sigma}, \hat{G}] = 0, \quad (1)$$

in which \mathbf{v}_F is vector Fermi velocity of the quasi-particles in the superconducting region and $\hat{\Sigma}$ is a self-energy term related to *e.g.* elastic and spin-flip scattering centers. In the contrast of real part of $\hat{\Sigma}$ which is an oscillatory function of energy, the imaginary part of the term is dissipative and decays when increasing the energy. Here, $\hat{\Delta}$ and $\hat{\tau}_3$ are defined as:

$$\hat{\Delta} = \begin{pmatrix} 0 & \tilde{\Delta} \\ \tilde{\Delta}^* & 0 \end{pmatrix}, \quad \tilde{\Delta} = \begin{pmatrix} 0 & \Delta \\ -\Delta & 0 \end{pmatrix}, \quad \hat{\tau}_3 = \begin{pmatrix} 1 & 0 \\ 0 & -1 \end{pmatrix}.$$

While \square and $\hat{\square}$ stand for 2×2 and 4×4 matrix quantities.

In experimental situations, the diffusive regime of transport is often reached as very clean (ballistic) samples may be hard

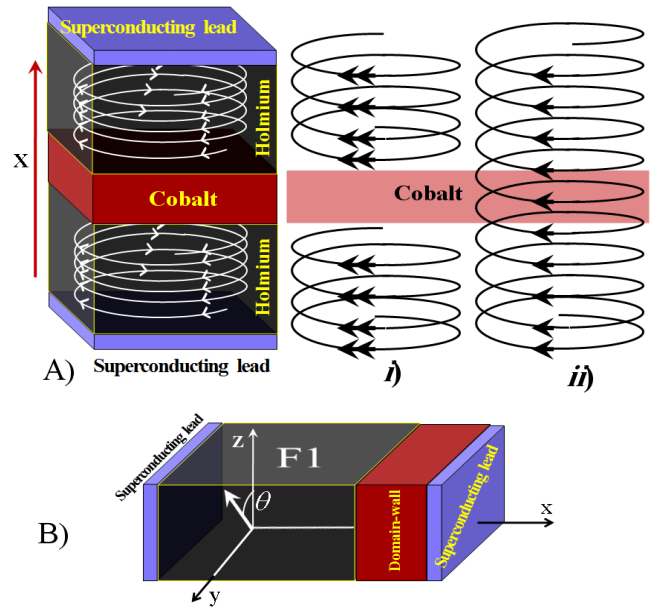


FIG. 1: (Color online) A): The schematic setup of a ferromagnetic trilayer of Ho|Co|Ho. The spiral curves show the trajectory of the magnetization vector in the Ho layer which rotates along a conical profile in the \hat{x} -direction. *i)* shows the configuration in which the magnetization patterns of the two Ho layers are completely identical, whereas in *ii)* the magnetization patterns follow a continuous spiral magnetization in the two Ho layers. B): Schematic model of the experimental setup of our proposed ferromagnetic Josephson junction including a domain-wall and homogeneous ferromagnetic layer which enables a controllable triplet-supercurrent. The angle θ represents the orientation of the homogeneous magnetization in the F1 layer with respect to the \hat{z} -direction.

to fabricate. In the diffusive limit, impurities in specimen are very strong and consequently the self-energy term $\hat{\Sigma}$ in the Eq. (2) dominates. The impurities will lead to randomization of the quasiparticle trajectories, scattering them all over k -space. By expanding the Green's function with respect to s - and p -wave spherical harmonics and performing an angular averaging process, one arrives at the Usadel-equation²⁸:

$$\nabla(\hat{G}\nabla\hat{G}) + \frac{i}{E_{th}}[E\hat{\rho}_3 + \text{diag}[\mathbf{h} \cdot \underline{\sigma}, (\mathbf{h} \cdot \underline{\sigma})^T], \hat{G}] = 0, \quad (2)$$

where $E_{th} = D/d_F^2$ is Thouless energy in which D is diffusive constant and d_F is length of ferromagnetic layer, h is exchange field of ferromagnetic region and $\hat{\rho}_3, \underline{\sigma}$ are Pauli matrixes which are available in Appendix A.

Throughout the paper, we shall assume that the ferromagnetic layer has been sandwiched between two conventional s -wave superconducting leads whose interfaces are located at $x = -d_F/2$ and $d_F/2$. Due to the isotropic superconducting order parameter and the impurity scattering, we may capture all the essential physics by considering an effective one dimensional system, thus $\nabla \equiv \partial/\partial x \equiv \partial_x$ in Eq. (2). For investigating the charge-current flowing through the system, we employ the following boundary conditions at the two contact regions with the superconducting reservoirs:

$$\begin{cases} 2\zeta \hat{G} \partial_x \hat{G} = [\hat{G}_{\text{BCS}}(\phi), \hat{G}] & x = -\frac{d_F}{2} \\ 2\zeta \hat{G} \partial_x \hat{G} = [-\hat{G}_{\text{BCS}}(-\phi), \hat{G}] & x = \frac{d_F}{2} \end{cases} \quad (3)$$

where \hat{G}_{BCS} is the bulk Green's function in the superconductors and ζ is defined as ratio between the resistance of the barrier region (R_B) and the resistance in the ferromagnetic film (R_F). We disregard here the influence of spin-dependent interfacial phase-shifts occurring at the interfaces since their effect is unimportant in the present context of an intrinsically inhomogeneous magnetization structure (including them would introduce slight shifts to the $0-\pi$ transition points).^{46,47}

For solving the Usadel equation and implementing boundary conditions numerically, it is convenient to parameterize the Green's function. There are two standard parameterizations approaches; θ - and Ricatti-parameterizations, and we will here employ the latter. The parameterized Green's function then reads as follows:

$$\hat{G} = \begin{pmatrix} \underline{N}(\underline{1} - \underline{\gamma}\tilde{\gamma}) & 2\underline{N}\underline{\gamma} \\ 2\underline{N}\tilde{\gamma} & \underline{N}(-\underline{1} + \underline{\gamma}\tilde{\gamma}) \end{pmatrix}. \quad (4)$$

By imposing a normalization condition for the Green's function, namely $\hat{G}^2 = \hat{1}$, \underline{N} and \underline{N} are obtained as

$$\underline{N} = \frac{1}{\underline{1} + \underline{\gamma}\tilde{\gamma}} \quad \underline{N} = \frac{1}{\underline{1} + \underline{\gamma}\tilde{\gamma}}. \quad (5)$$

Within the Ricatti-parametrization scheme, the components of the bulk superconductor Green's function are:

$$\begin{aligned} \gamma_{\text{BCS}}(\phi) &= i\tau_2 s / (1 + c) e^{i\phi/2}, \\ \tilde{\gamma}_{\text{BCS}}(\phi) &= \gamma_{\text{BCS}}(\phi) e^{-i\phi}, \end{aligned} \quad (6)$$

where ϕ is superconducting phase difference between the two s -wave superconducting leads and s, c is defined as $\sinh \vartheta$ and $\cosh \vartheta$, respectively, in which $\vartheta = \text{atanh}(\Delta(T)/E)$. We use standard BCS temperature dependent of superconducting gap in our calculations and $\Delta_0 = \Delta(0)$ stands for superconducting gap in the absolute zero. Throughout the paper we normalize all energies with respect to superconducting gap at the zero temperature (Δ_0) and all lengths with respect to ferromagnetic layer length. We use units so that $\hbar = k_B = 1$.

For investigating the electronic transport properties of all configurations one needs to obtain the Keldysh block of the Green's function. Under equilibrium conditions, the Keldysh component can be obtained from the Retarded and Advanced blocks as $\hat{G}^K = (\hat{G}^R - \hat{G}^A) \tanh(E/2k_B T)$ and $\hat{G}^A = -(\hat{\rho}_3 \hat{G}^R \hat{\rho}_3)^\dagger$. The charge-current is then obtained via:

$$\frac{I_C}{I_{0C}} = \left| \int_{-\infty}^{+\infty} dE \text{Tr} \left\{ \hat{\rho}_3 \left(\hat{G} \partial_x \hat{G} \right)^K \right\} \right| \quad (7)$$

in which $I_{0C} = N_0 e D / 16 d_F$, N_0 is the normal density of states per spin. Above, $\left(\hat{G} \partial_x \hat{G} \right)^K$ denotes the Keldysh component of the $\hat{G} \partial_x \hat{G}$ matrix. We now proceed to study the

transport properties of several experimentally accessible configurations, in particular pertaining the experiment by Robinson *et al.*³⁵. We underline once more that our approach grants us access to the full proximity regime in addition to complicated magnetization textures which cannot be treated analytically.

3. SPIN-TRIPLET SUPERCURRENT THROUGH A FERROMAGNETIC HO|CO|HO TRILAYER

In this section, we present main results of the paper: a theoretical investigation of a ferromagnetic Ho|Co|Ho trilayer sandwiched between two s -wave superconductors, as recently experimentally studied in Ref. 35. The magnetization structure of isolated Ho is experimentally known⁴³ and depicted in portion A) of Fig. 1. Analytically, the instantaneous direction of the local magnetization can thus be written as:

$$\begin{aligned} \mathbf{h} &= h (\cos \alpha \hat{x} + \Xi \sin \alpha) \\ \Xi &= \{ \sin(Qx) \hat{y} + \cos(Qx) \hat{z} \}, \end{aligned} \quad (8)$$

where $Q = 2\pi/\lambda$ and λ is the spiral length in Ho. In Ref. 35, this was estimated to $\lambda \simeq 3.4$ nm. The apex angle is denoted by α and equals $4\pi/9$.^{35,43} For both Ho and Co ferromagnetic layers, the strength of the exchange field is larger than alloys and compounds of Pd and Ni. For $\text{Pd}_x\text{Ni}_{1-x}$ alloys, weak strengths of the exchange field in the range of $h/\Delta_0 \approx 5-10$ are accessible in the experiments. This should be contrasted with intrinsically ferromagnetic materials whose exchange field strengths are often very large (100 meV – 1 eV). We set superconducting coherent length as $\xi_S = 15$ nm which is accessible for example in Nb. For more stability in the numerical code, we add an imaginary part to the quasiparticle energies equal to $\delta/\Delta_0 = 5 \times 10^{-2}$ which modeling inelastic scattering in the specimen. To simulate numeri-

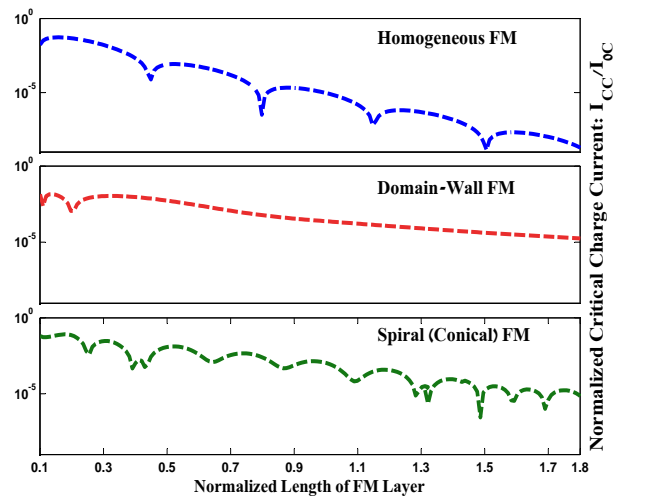


FIG. 2: (Color online) The normalized critical charge current for three types of magnetization textures. Top, middle and bottom frames show critical supercurrent through sandwiched uniform, domain-wall and spiral ferromagnetic layers, respectively.

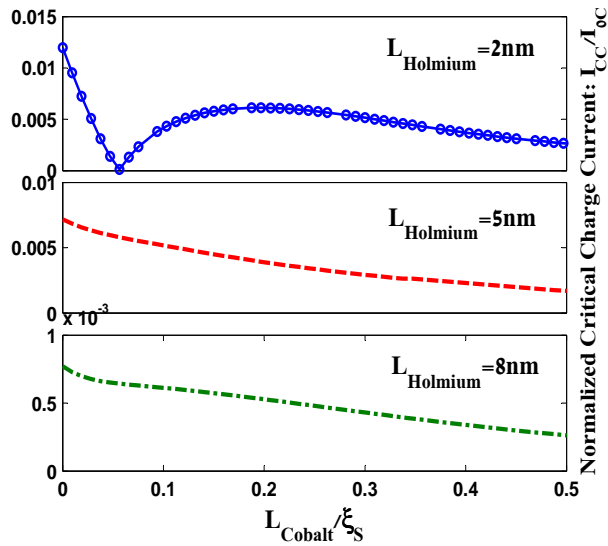


FIG. 3: (Color online) The normalized critical supercurrent through a magnetic Ho|Co|Ho trilayer vs. the length of the Co layer for three values of Ho-layer lengths, $L_{\text{Ho}}=2$ nm, 5 nm and 8 nm.

cally the ferromagnetic trilayer sandwiched between the two s -wave superconducting leads, we should first note the parameter regime in which the quasi-classical Green's function method is valid. Due to the requirement of the Fermi energy being much larger than all energy scales, we set $\hbar/\Delta_0 = 80$ to model a strong exchange field still within the regime of validity. Throughout our calculations, we fix the temperature at $T/T_c = 0.2$ and also set the ratio of barrier and ferromagnetic resistances to $\zeta = R_B/R_F = 5$. For the value of the exchange field considered here, it can be shown that the spin-dependent phase-shifts occurring at the interface may be neglected.

To begin with, we mention briefly the qualitative difference between having a homogeneous and inhomogeneous magnetization in the magnetic layer. In Fig. 2, we show the critical charge current behavior vs. the thickness of ferromagnetic layer for three scenarios: a homogeneous exchange field, a domain-wall ferromagnet, and finally a spiral (conical) magnetization texture. As seen, the fundamental difference between the homogeneous case in the upper panel of Fig. 2 and the two inhomogeneous scenarios is that the current becomes long-ranged in the latter cases, i.e. the critical supercurrent decays on a much larger length-scale compared to the homogeneous case. This is due to the generation of a long-range triplet supercurrent which is sustained by the inhomogeneous field^{2,14,23,40,42}. Moreover, the spiral magnetization pattern gives rise to a rapid oscillation pattern superimposed on the $0-\pi$ transitions, as was shown in Refs. 33,34.

Now we model the ferromagnetic Ho|Co|Ho trilayer by:

$$\mathbf{h} = \begin{cases} h (\cos \alpha \hat{x} + \Xi \sin \alpha) & x < -\frac{L_{\text{Co}}}{2} \\ h \hat{z} & -\frac{L_{\text{Co}}}{2} < x < \frac{L_{\text{Co}}}{2} \\ h (\cos \alpha \hat{x} + \Xi \sin \alpha) & x > \frac{L_{\text{Co}}}{2} \end{cases}, \quad (9)$$

where we assume that the middle of the Co-layer is located at $x = 0$. In Fig. 3, we show the variations of the critical super-

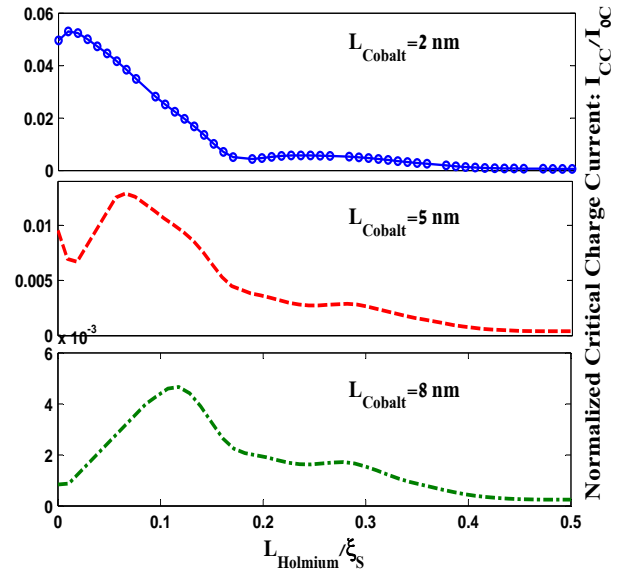


FIG. 4: (Color online) The normalized critical supercurrent through a ferromagnetic trilayer of Ho|Co|Ho vs. the length of the Ho layer for three values of Co-layer lengths, $L_{\text{Co}}=2$ nm, 5 nm and 8 nm.

current when the Co-layer length is varying [see portion A) of Fig. 1 for the structure under consideration]. Results are provided for three distinct values of the Ho-layers length. We first assume that the Ho-layers have identical spiral magnetization patterns. As we shall see later, the results for the critical current are sensitive to the exact magnetization texture in the Ho-layers. The magnetization of the Co-layer is taken to be along the \hat{z} -axis, i.e. parallel with the contact-interfaces, as should be reasonable for a thin-film structure. As seen in Fig. 3, for thin Ho-layers, the critical supercurrent displays only one $0-\pi$ transition point. For larger values of L_{Ho} , the supercurrent decays monotonically similar to flowing critical supercurrent through an S|N|S junction where only spin-singlet condensation contributes to the supercurrent. This is consistent with the experimental observation by Robinson *et al.*³⁵. For thick Ho-layers, the charge supercurrent thus behaves as if a normal layer has been sandwiched between two s -wave superconducting. The long decay length of the supercurrent, comparable to a normal Josephson junction, is evidence of precisely a long-ranged spin-triplet supercurrent flowing through the ferromagnetic Ho|Co|Ho trilayer.

Next, we investigate how the current behaves upon altering the Ho-layer thickness. We show results for three distinct values of L_{Co} in Fig. 4. The Co-layer exchange field is as before assumed to be oriented parallel to the interface regions. As seen, the current now decays in a non-monotonic fashion. Interestingly, Robinson *et al.*³⁵ observed a set of anomalous sharp peaks in the current when L_{Ho} is increasing. Although we are not able to reproduce such sharp peaks within this quasi-classical treatment, we confirm the non-monotonic dependence of the critical current observed by Ref. 35. In order to investigate further if the specific magnetization profile is crucial with regard to the appearance of the anomalous behavior observed experimentally, we investigate a slightly different

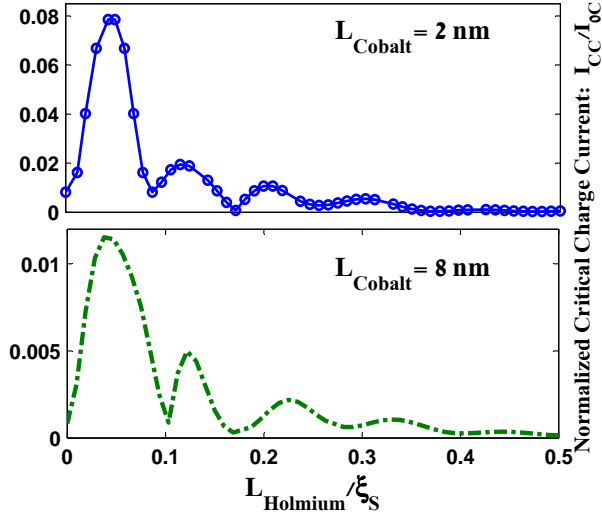


FIG. 5: (Color online) The normalized critical supercurrent through a trilayer of Ho|Co|Ho vs. the length of the Ho layer for two values of Co-layer lengths, $L_{Co}=2$ nm and 8 nm. In this case, we assume that the magnetization vector in Ho layers follow a continuous spiral pattern without being interrupted by the Co layer.

magnetization texture model in the Ho-layers. Whereas the magnetization pattern previously was assumed to be identical in both layers, we show in Fig. 5 results for the case when the magnetization pattern in the right Ho layer couples continuously to the left layer as if the Co-layer has no influence on it [see part *ii*) of portion A) of Fig. 1]. Unlike the first case, several minima now appear in the critical supercurrent, out of which two are $0-\pi$ transition points while the others are local minima. *This demonstrates that the exact behavior of the supercurrent is sensitive to the specific magnetization profile in the inhomogeneous magnetic layers.* Motivated by this finding, we explore in the next section how the results change when the Ho-layers are replaced by domain-wall ferromagnets.

4. SPIN-TRIPLET SUPERCURRENT THROUGH A FERROMAGNETIC STRUCTURE WITH DOMAIN-WALLS

We keep the same parameters as used in the previous section, but now replace the spiral magnetization patterns in portion A) of Fig. 1 with domain-wall ferromagnets. Both a Neel and Bloch-wall configuration have been investigated by us numerically, and were found to give virtually identical results for the charge-current transport. Thus, we here present results only for the Bloch domain-wall case. Fig. 6 shows the critical charge-current through a ferromagnetic trilayer with the following magnetization structure:

$$\mathbf{h} = \begin{cases} h(\cos \beta \hat{y} + \sin \beta \hat{z}) & x < -\frac{L_{Co}}{2} \\ h \hat{z} & -\frac{L_{Co}}{2} < x < \frac{L_{Co}}{2} \\ h(\cos \beta \hat{y} + \sin \beta \hat{z}) & x > \frac{L_{Co}}{2} \end{cases} \quad (10)$$

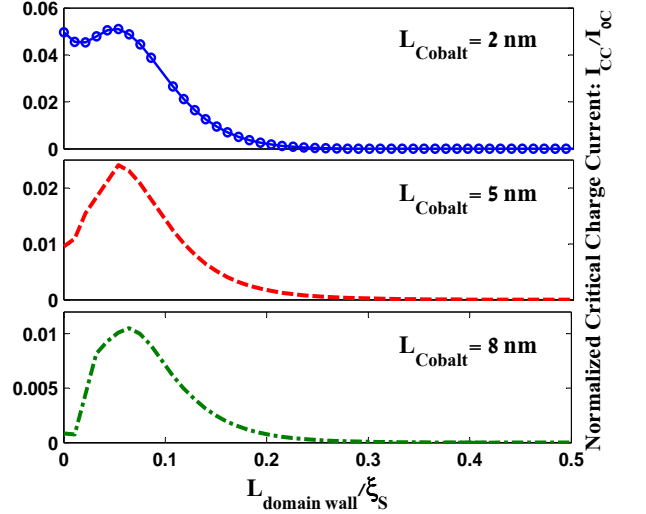


FIG. 6: (Color online) The normalized critical supercurrent through sandwiched Bloch-wall|Co|Bloch-wall trilayer vs length of Bloch-wall layers for three different values of Co layer lengths, $L_{Co}=2$ nm, 5 nm and 8 nm. Here magnetization direction of Co layer is along the \hat{z} -axes.

where d_W is width of domain-wall and:

$$\beta = -2\text{atanh}\left(\frac{x - L_d/2}{d_W}\right). \quad (11)$$

We set $d_W=L_d/2$ throughout our computations, and provide results for the critical supercurrent biased through the trilayer vs. the domain-wall-layer length L_d for three distinct values of the Co-layer lengths in Fig. 6. For $L_{Co} = 2$ nm the critical supercurrent features two $0-\pi$ transition points and these transition points disappear when L_{Co} increases. This finding coincides with the Ho|Co|Ho trilayer. As can be seen from Fig. 6, the variation of critical supercurrent vs. the length of domain-wall-layer shows a non-monotonic behavior, as in Fig. 4. In effect, domain-wall ferromagnets can serve a similar purpose as Ho with regard to the generation of a long-range current.

Due to the somewhat complicated magnetization texture in the trilayer structure considered in Ref. 35, it is tempting to consider if it is possible to simplify the structure of the magnetic layers and still obtain a setup where the triplet supercurrent can be experimentally controlled. In Ref. 15, a magnetic trilayer consisting of homogeneous, misaligned ferromagnets was proposed as a setup where the long-range current could be controlled by varying the angle of misalignment. Experimentally, it would nevertheless be highly challenging to exert individual control over the local magnetization field in each layer via application of external fields. We here propose another type of heterostructure which might be more beneficial in this regard. As is seen in part B) of Fig. 1, we consider a superconductor|domain-wall|ferromagnet|superconductor junction where the coercive field of the homogeneous ferromagnet is sufficiently low to allow tuning of its magnetization via an external field without altering the domain-wall ferromagnet. In this way, the

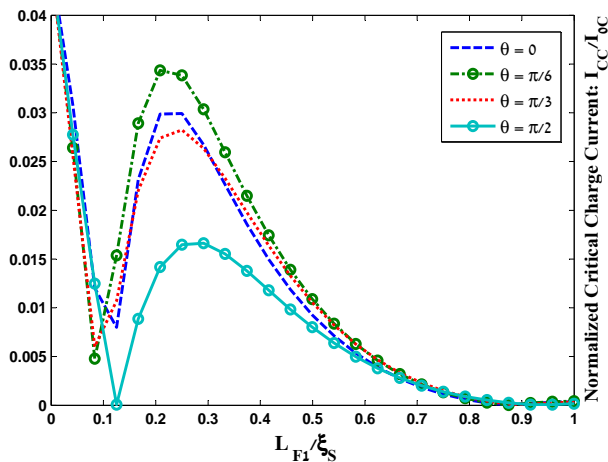


FIG. 7: (Color online) The normalized critical supercurrent through our proposed Bloch-wall|homogeneous ferromagnetic bilayer vs. the length of homogeneous ferromagnetic layer L_{F1} for four values of magnetic orientation angle of homogeneous ferromagnet with respect to \hat{z} -direction, $\theta=0, \pi/6, \pi/3$ and $\pi/2$.

domain-wall ferromagnet serves as a source for the long-range triplet current, while the orientation of the homogeneous ferromagnet can tune this contribution. We define the magnetic field orientation angle of the F1 layer as θ (see Fig. 1, portion B)), and thus the magnetization profile of the ferromagnetic layer reads:

$$\mathbf{h} = \begin{cases} h_1(\cos \theta \hat{z} + \sin \theta \hat{y}) & x < L_{F1} \\ h_2(\cos \beta \hat{y} + \sin \beta \hat{z}) & x > L_{F1} \end{cases}. \quad (12)$$

As before, we set the exchange field in the homogeneous ferromagnetic region to $h_1/\Delta_0 = 15$ whereas it is stronger in the domain-wall region $h_2/\Delta_0 = 70$ to avoid influence of the magnetic field on the domain-wall region. The width of the domain-wall is here set to $L_d = 3.4$ nm, and we show the results for the critical supercurrent in Fig. 7 for four values of magnetic field orientation angle of the F1 layer, $\theta=0, \pi/6, \pi/3$, and $\pi/2$. It is seen that the current is enhanced from $\theta=0$ up to values approximately near $\theta=\pi/6$, suggesting that the triplet contribution to the current is tuned. The reason for this is that a singlet supercurrent would be completely invariant under a rotation of the exchange field since such a current is spinless. By increasing value of the angle further from $\theta=\pi/6$ up to $\pi/2$, the critical supercurrent is suppressed. The main advantage of this setup compared to *e.g.* the trilayer structure considered in Ref. 15 is that only one ferromagnetic layer needs to have its magnetization orientation tuned, which is experimentally more feasible than individually controlling the magnetization structure of each individual layer in a trilayer structure.

5. SUMMARY

We have investigated the possibility of establishing a long-range spin-triplet supercurrent through an inhomogeneous ferromagnetic region consisting of a Ho|Co|Ho trilayer sandwiched between two conventional s -wave superconductors. Utilizing a full numerical solution in the diffusive regime of transport, the behavior of the supercurrent in several relevant configurations of the magnetic trilayer has been obtained. We find qualitatively very good agreement with the recently reported experimental results by Robinson *et al.*³⁵ regarding the behavior of the supercurrent as a function of the width of the Co-layer. Moreover, we find a synthesis of $0-\pi$ oscillations with superimposed rapid oscillations when varying the width of the Ho-layer. We are not able to reproduce the anomalous peaks observed experimentally in this regime, but note that the results obtained are quite sensitive to the exact magnetization profile in the Ho-layers. We also investigate the supercurrent in a system where the intrinsically inhomogeneous Ho ferromagnets are replaced with domain-wall ferromagnets, and find similar behavior as in the Ho|Co|Ho setup. In addition, we propose a novel type of ferromagnetic Josephson junction involving a domain-wall and homogeneous ferromagnet which could be used to obtain a controllable spin-triplet supercurrent. The advantageous of our proposed structure compared to the structure considered in Ref. 15 is a simpler magnetic profile which could be beneficial from an experimental point of view.

Acknowledgement

We thank J. W. A. Robinson for very useful discussions, and appreciate support from the Physics department computer center of Isfahan University.

Appendix A: Pauli matrixes

The Pauli matrixes we use in this paper

$$\begin{aligned} \underline{\tau}_1 &= \begin{pmatrix} 0 & 1 \\ 1 & 0 \end{pmatrix}, \quad \underline{\tau}_2 = \begin{pmatrix} 0 & -i \\ i & 0 \end{pmatrix}, \quad \underline{\tau}_3 = \begin{pmatrix} 1 & 0 \\ 0 & -1 \end{pmatrix}, \\ \underline{\hat{1}} &= \begin{pmatrix} 1 & 0 \\ 0 & 1 \end{pmatrix}, \quad \underline{\hat{1}} = \begin{pmatrix} 1 & 0 \\ 0 & 1 \end{pmatrix}, \quad \underline{\hat{\tau}}_i = \begin{pmatrix} \tau_i & 0 \\ 0 & \tau_i \end{pmatrix}, \\ \underline{\hat{\rho}}_1 &= \begin{pmatrix} 0 & \tau_1 \\ \tau_1 & 0 \end{pmatrix}, \quad \underline{\hat{\rho}}_2 = \begin{pmatrix} 0 & -i\tau_1 \\ i\tau_1 & 0 \end{pmatrix}, \quad \underline{\hat{\rho}}_3 = \begin{pmatrix} 1 & 0 \\ 0 & -1 \end{pmatrix}. \end{aligned} \quad (A1)$$

¹ A. I. Buzdin, Rev. Mod. Phys. **77**, 935 (2005).

² F. S. Bergeret, A. F. Volkov and K. B. Efetov, Rev. Mod. Phys. **77**, 1321 (2005).

³ A. A. Golubov, M. Y. Kupriyanov and E. Il'ichev, Rev. Mod. Phys. **76**, 411 (2004).

⁴ M. L. Della Rocca, M. Aprili, T. Kontos, A. Gomez, and P.

- Spathis, Phys. Rev. Lett. **94**, 197003 (2005).
- ⁵ T. Kontos, M. Aprili, J. Lesueur, X. Grison, and L. Dumoulin Phys. Rev. Lett. **93**, 137001 (2004).
- ⁶ T. S. Khaire, M. A. Khasawneh, W. P. Pratt, Jr., and N. O. Birge, Phys. Rev. Lett. **104**, 137002 (2010).
- ⁷ H. Z. Arham, T. S. Khaire, R. Loloee, W. P. Pratt, Jr., and N. O. Birge Phys. Rev. B **80**, 174515 (2009).
- ⁸ T. S. Khaire, W. P. Pratt, Jr., and N. O. Birge Phys. Rev. B **79**, 094523 (2009).
- ⁹ Y. Asano, Y. Sawa, Y. Tanaka, and A. A. Golubov Phys. Rev. B **76**, 224525 (2007).
- ¹⁰ Y. Asano, Y. Tanaka, T. Yokoyama, and S. Kashiwaya Phys. Rev. B **74**, 064507 (2006).
- ¹¹ T. Klapwijk Nature Physics **6**, 329 (2010).
- ¹² J. Wang, M. Singh, M. Tian, N. Kumar, B. Liu, C. Shi, J. K. Jain, N. Samarth, T. E. Mallouk and M. H. W. Chan, Nat. Phys. **6**, 389 (2010).
- ¹³ J. Linder, T. Yokoyama, A. Sudbø and M. Eschrig, Phys. Rev. Lett. **102**, 107008 (2009).
- ¹⁴ M. Eschrig, T. Löfwander, Nat. Phys. **4**, 138 (2008).
- ¹⁵ M. Houzet and A. I. Buzdin, Phys. Rev. B **76** 060504(R) (2007).
- ¹⁶ G. Mohammadkhani and M. Zareyan Phys. Rev. B **73**, 134503 (2006).
- ¹⁷ E. Goldobin, D. Koelle, R. Kleiner, and A. Buzdin Phys. Rev. B **76**, 224523 (2007).
- ¹⁸ A. Buzdin Phys. Rev. Lett. **101**, 107005 (2008).
- ¹⁹ A. Buzdin and A. E. Koshelev Phys. Rev. B **67**, 220504 (2003).
- ²⁰ F. S. Bergeret, A. F. Volkov, and K. B. Efetov Phys. Rev. Lett. **86**, 3140 (2001).
- ²¹ F. S. Bergeret, A. F. Volkov, and K. B. Efetov Phys. Rev. Lett. **86**, 4096 (2001).
- ²² F. S. Bergeret, A. F. Volkov, and K. B. Efetov Phys. Rev. B **64**, 134506 (2001).
- ²³ A. F. Volkov and K. B. Efetov Phys. Rev. B **81**, 144522 (2010).
- ²⁴ A. F. Volkov and K. B. Efetov Phys. Rev. B **78**, 024519 (2008).
- ²⁵ A. F. Volkov, A. Anishchanka, and K. B. Efetov Phys. Rev. B **73**, 104412 (2006).
- ²⁶ I. B. Sperstad, J. Linder, and A. Sudbø Phys. Rev. B **78**, 104509 (2008).
- ²⁷ D. Sprungmann, K. Westerholt, H. Zabel, M. Weides, and H. Kohlstedt, Phys. Rev. B **82**, 060505 (2010).
- ²⁸ K. Usadel, Phys. Rev. Lett. **25**, 507 (1970).
- ²⁹ G. D. Mahan, Many Body Physics (Kluwer, New York, 2000).
- ³⁰ E. M. Lifshitz, and L. P. Pitaevskii, Physical Kinetics (Pergamon, Oxford, 1981).
- ³¹ V. Chandrasekhar, Chapter in *The Physics of Superconductors*, Vol. II, edited by Bennemann and Ketterson (2004).
- ³² G. Eilenberger, Z. Phys. **214**, 195 (1968).
- ³³ M. Alidoust, J. Linder, G. Rashedi, T. Yokoyama, and A. Sudbø, Phys. Rev. B **81**, 014512 (2010).
- ³⁴ G. B. Hala'sz, J. W. A. Robinson, J. F. Annett, and M. G. Blamire, Phys. Rev. B **79**, 224505 (2009).
- ³⁵ J. W. A. Robinson, J. D. S. Witt and M. G. Blamire, Science, **329**, 5987 (2010).
- ³⁶ L. N. Bulaevskii, V. V. Kuzii, and A. A. Sobyenin, Pisma Zh. Eksp. Teor. Fiz. **25**, 314 (1977) [JETP Lett. **25**, 290 (1977)].
- ³⁷ V. V. Ryazanov, V. A. Oboznov, A. Yu. Rusanov, A. V. Veretennikov, A. A. Golubov, and J. Aarts, Phys. Rev. Lett. **86**, 2427 (2001).
- ³⁸ Ya. M. Blanter and F. W. J. hekking, Phys. Rev. B **69**, 024525 (2004).
- ³⁹ B. Crouzy, S. Tollis, and D.A. Ivanov, Phys. Rev. B **75**, 054503 (2007).
- ⁴⁰ K. Halterman, O. T.valls and P. H.Barsic, Phys. Rev. B **77**, 174511 (2008).
- ⁴¹ K. Halterman, P. H.Barsic and O. T.valls Phys. Rev. Lett. **99**, 127002 (2007).
- ⁴² L. Trifunovic and Z. Radovic, Phys. Rev. B **82**, 020505 (2010).
- ⁴³ I. Sosnin, H. Cho, V. T. Petrashov, and A. F. Volkov Phys. Rev. Lett. **96** 157002 (2006).
- ⁴⁴ R. S. Keizer, S. T. B. Goennenwein, T. M. Klapwijk, G. Miao, G. Xiao, and A. Gupta, Nature (london) **439**, 825 (2006).
- ⁴⁵ J.W. A. Robinson, Gabor B. Halasz, A. I. Buzdin, and M. G. Blamire Phys. Rev. Lett. **104**, 207001 (2010).
- ⁴⁶ D. Huertas-Hernando, Y. Nazarov, and W. Belzig, Phys. Rev. Lett. **88**, 047003 (2002).
- ⁴⁷ A. Cottet and W. Belzig, Phys. Rev. B **72**, 180503 (2005).